A Vision-based Line Following Strategy for an Autonomous UAV

Alexandre S. Brandão[1], Felipe N. Martins[2] and Higor B. Soneguetti[2]

[1]*Robotics Specialization Group (NERO), Dep. of Electrical Engineering, Federal University of Viçosa, Brazil*
[2]*Institute of Engineering, Hanze University of Applied Sciences, Groningen, Netherlands**

Keywords: Unmanned Aerial Vehicles, Nonlinear Control, Vision-based Control, Quadrotor.

Abstract: Unmanned Aerial Vehicles (UAVs) are versatile machines that can be used in a variety of applications, such as automatic monitoring of crops and water channels, pest detection, animal counting etc. Autonomous flying is a desirable feature for UAVs, especially for those that are frequently used in monitoring and inspection of large areas. In some situations, global positioning system signal is not guaranteed or its error might be too large, hence other methods of local position feedback are required. In such a context, we present the development of a vision-based line following strategy for an autonomous UAV. The proposed system is intended to guide an autonomous UAV to follow water channel margins, crop lines and other similar patterns, to support automatic monitoring and inspection activities. We present the design of a nonlinear path following controller and we show that the resulting closed-loop system is stable in the sense of Lyapunov. We also propose a visual-based line detection algorithm that it is capable of detecting the average position and orientation of the main lines on the image frames captured by the UAV downwards facing camera. Finally, we present and discuss some experimental results that show the good performance of the proposed system.

1 INTRODUCTION

According to estimates of the United Nations Food and Agriculture Organization (FAO), in the next 40 years the world population will reach 8.5 billion people. In this scenario, the area available for food production tends to be reduced, which means that it is extremely important to aim the development of systems to better utilize it. Systems that are focused on increase productivity of agricultural goods are part of the so-called precision agriculture. Unmanned Aerial Vehicles (UAVs) can contribute with the development of precision agriculture on applications like automatic monitoring of crops, application of pesticides, pest detection, among others. One example of such application is presented in (Tokekar et al., 2013), that proposes a system that deals with the problem of co-ordinated planning for a UAV and a ground mobile robot to measure the level of nitrogen over a farm in order to optimize fertilizer application. The authors argue that the ability to calculate the proper amount of fertilizer to be applied can dramatically reduce its use, which is desirable from environmental and economic perspectives.

---

*Dr. Martins is on leave from the Federal Institute of Espirito Santo - Campus Serra - Robotics and Automation Research Group (NERA), Brazil

Autonomous UAVs commonly rely on Global Positioning System (GPS) to acquire instantaneous position information. In a monitoring application, GPS coordinates might be used as reference way-points for the UAV to follow. However, the accuracy of GPS position measurements is influenced by several conditions, such as atmospheric effects, satellite clock errors, receiver electronics etc., which results in a typical accuracy of about 5 to 15m, on average, for civilian GPS horizontal position fixes (Roebuck, 2012). In some applications like channel or crop monitoring on a low altitude flight, such error is too large meaning GPS signals cannot be used as the only source of information for the UAV controller. Inertial sensors (like accelerometers and gyroscopes) can also be used to provide odometry information, but this information suffers from drifting due to accumulation of measurement errors. Therefore, other methods of local position feedback are required for the UAV to accurately follow the desired path, while GPS fixes could be used as a general guide towards the correct position.

Several researchers have proposed vision-based systems to control quadrotors UAVs. For example, in (Venugopalan et al., 2012) the application of ocean monitoring is considered. The authors present a control system for automatic landing of a quadrotor on an boat using information acquired by a downwards camera mounted on the UAV. By its turn, in (Warren

et al., 2015) the authors deal with the problem of long-range stereo visual odometry for UAVs. They argue that navigating via vision reduces dependence on GPS and other global navigation satellite systems, enhancing navigation robustness in low altitude applications ($< 120m$) even in the presence of jamming, spoofing or long dropouts. Finally, a visual-based control system to guide an autonomous aerial vehicle was presented in (Sotomayor et al., 2014) to be applied on crop inspection. The orientation of the crop lines for the UAV to follow is extracted by a computer vision method based on the oriented textures. The angle obtained by the vision system is the reference for the PID controllers that guide the UAV. The authors have presented simulation results to show the viability of their proposed system.

The system we propose in the present paper follows the same general idea of the one presented in (Sotomayor et al., 2014), i.e., the UAV must follow a line which is oriented according to the main orientation of the lines on the surface. The main orientation of the lines is extracted by a computer vision algorithm and its angle and position are used as reference for the UAV path-following controller. The main differences of our strategy with respect to the one presented in (Sotomayor et al., 2014) are: (1) instead of using two PID controllers we propose the use of a nonlinear coupled controller to drive the UAV throughout the path; (2) we show that the resulting system is asymptotically stable in the sense of Lyapunov; (3) we propose a different method to detect the orientation of the main lines on the image; and (4) we show experimental results of the line detection algorithm on a real video from a quadrotor downwards camera while flying outdoors over different surfaces. Besides its application on precision agriculture, other possible applications of the proposed system include carrying instruments to monitor the conditions of water channels, rivers, roads, transmission lines, among others.

2 QUADROTOR MODEL

In this paper we are going to consider the model of a quadrotor, which is the UAV used during the experiments. A quadrotor is a kind of helicopter that has four rotors disposed at the ends of a cross-shaped structure. Two of its rotors rotate in clockwise direction while the others rotate in counterclockwise direction. The quadrotor motion is controlled by varying the speed of each individual rotor. The variation in speed of each rotor results in turning or tilting that allows the quadrotor to move in any direction in space

or rotate around its own reference system.

The pose of the vehicle in the 3-D space is represented in generalized coordinates by ${}^e\mathbf{q} = \begin{bmatrix} {}^e\xi & {}^e\eta \end{bmatrix}^T$, where ${}^e\xi = \begin{bmatrix} x & y & z \end{bmatrix}^T \in \mathbb{R}^3$, corresponds to the longitudinal, lateral and normal displacements in the inertial frame $\langle e \rangle$, and ${}^s\eta = \begin{bmatrix} \phi & \theta & \psi \end{bmatrix}^T \in \mathbb{R}^3$, corresponds to the angles of roll, pitch and yaw with respect to the spatial frame $\langle s \rangle$. Notice that $\langle s \rangle$ has the same orientation of $\langle e \rangle$, and thus ${}^s\eta \equiv {}^e\eta$. Fig. 1 illustrates the reference frames and the abstract control inputs f_1, f_2, f_3 and f_4 for a quadrotor.

Differently from other works found in the literature, the motors of the quadrotor shown in Fig. 1 are not aligned with the $x-$ and $y-$ axis of its body frame. In turn, they are rotated of 45 degrees, which means that any lateral or longitudinal maneuver requires a joint action of all motors. This is the case of the AR.Drone quadrotor, which is the UAV we used in our experiments.

The vector of forces applied in the body frame is given by

$$\mathbf{f} = \begin{bmatrix} f_x \\ f_y \\ f_z \end{bmatrix} = \begin{bmatrix} 0 \\ 0 \\ \sum_{i=1}^4 f_i \end{bmatrix}, \quad (1)$$

where f_i is the thrust produced by each motor, which is proportional to the square of angular velocity, i.e., $f_i = C_f \omega^2$. C_f depends on parametric constants associated to the number of rotor blades, width and shape of the vanes, inner and outer radius of the air flow by the impeller, air density, among other aerodynamic constants.

Now, the vector of torques applied in the body frame is represented as

$$\tau = \begin{bmatrix} \tau_\phi \\ \tau_\theta \\ \tau_\psi \end{bmatrix} = \begin{bmatrix} k_1 & k_1 & -k_1 & -k_1 \\ -k_1 & k_1 & k_1 & -k_1 \\ k_2 & -k_2 & k_2 & -k_2 \end{bmatrix} \begin{bmatrix} f_1 \\ f_2 \\ f_3 \\ f_4 \end{bmatrix}, \quad (2)$$

where k_1 is the distance between the reference axis and the point where each force is applied, and k_2 represents the relationship between the torque generated by the engine and its corresponding thrust.

Considering a camera attached to the quadrotor body frame, any roll or pitch maneuver will also rotate the camera frame. As a result, if the UAV is using its downwards camera information to locate a target or a line to be followed, the information about its own orientation needs to be used to compensate for the image displacement. If the purpose of navigation is to follow a line in the center of the image plane, a roll or pitch rotation of the camera frame will be problematic. For instance, let us consider the line-following problem. Let us assume that the quadrotor

needs to follow a line painted on the ground with constant forward speed. Suppose the vehicle detects its actual position is to the left of the line, and so its controller generates a command to move it to the right. For a regular quadrotor to move to the right it needs to first roll so that the resulting force **f** has a component pointing at the *y* direction. Therefore, the act of trying to move right (by rolling) will make the line painted on the ground apparently move even more to the right on the image captured by the camera. This means that the apparent error increases even more, which is not desirable.

In our proposal, the central line in the image plane is represented by a threshold between sidewalks and streets, between grass and water channels, or between planted area and pathways, and so on. Therefore, for the vision-based line following system to work properly it is necessary to keep the image frame parallel to the ground frame. This can be accomplished by mounting the downwards camera on a frame that compensates for the roll and pitch angles, maintaining the camera frame aligned with the ground surface.

Another way to keep the image frame parallel to the ground during navigation is to use a holonomic system, which, in terms of control, is capable to modify any state variable without affecting any other. For instance, consider the vehicle shown in Figure 1 and note that a longitudinal *x* (or lateral *y*) displacement requires a pitch θ (or roll ϕ) maneuver. Thus the pair are strongly coupled. Now, compare it with the vehicle shown in Figure 2 and notice that such coupling is not present. For its motor configuration, the vector of forces applied in the body frame is given by

$$\mathbf{f} = \begin{bmatrix} \dfrac{\sin\beta}{\sqrt{2}}(-f_1 + f_2 + f_3 - f_4) \\ \dfrac{\sin\beta}{\sqrt{2}}(-f_1 - f_2 + f_3 + f_4) \\ \cos\beta \sum_{i=1}^{4} f_i \end{bmatrix}, \quad (3)$$

where β is the tilt angle of the motor with respect to the $z-$ axis of the body frame.

In addition, the vector of torques applied in the body frame is represented as

$$\tau = \cos\beta \begin{bmatrix} k_1 & k_1 & -k_1 & -k_1 \\ -k_1 & k_1 & k_1 & -k_1 \\ k_2 & -k_2 & k_2 & -k_2 \end{bmatrix} \begin{bmatrix} f_1 \\ f_2 \\ f_3 \\ f_4 \end{bmatrix}, \quad (4)$$

The tilt angle introduced in this model increases the maneuverability of the rotorcraft. According to (Raffo et al., 2011), this makes possible an horizontal displacement without the necessity to employ an augmented state vector nor cascade control strategies. Therefore, such a vehicle would be suitable for
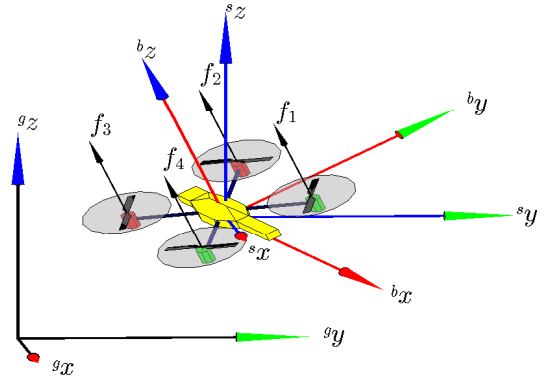

Figure 1: CAD model of a quadrotor, with the reference frames and abstract control inputs f_i associated to them. The spatial, ground and body frames are denoted by $\langle s \rangle$, $\langle g \rangle$ and $\langle b \rangle$, respectively.
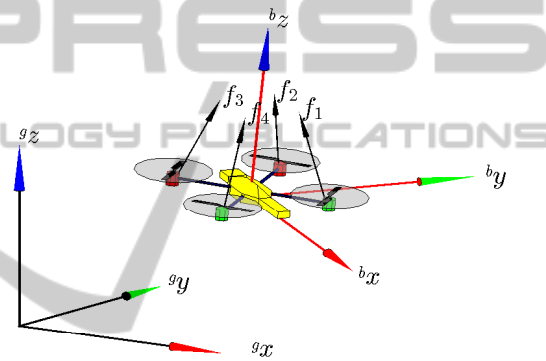

Figure 2: CAD model of a quadrotor with tilted propellers.

our proposed system without the necessity of mounting the downwards camera onto a gimbal stabilizing frame. However, the augmented maneuverability comes with an expense of an increase in energy consumption. For example, when the quadrotor is hovering at a fixed position, the horizontal components of the forces generated by the propellers need to be cancelled out. Therefore, energy is lost during a hovering maneuver just to guarantee stationary flight.

In this work we consider only the case of flat surfaces and we assume that the inner controller of the UAV maintains the aircraft in a desired vertical quota. In this case, for both types of quadrotors the kinematic model is given by

$$\begin{bmatrix} \dot{x} \\ \dot{y} \\ \dot{\alpha} \end{bmatrix} = \begin{bmatrix} \cos\alpha & -\sin\alpha & 0 \\ \sin\alpha & \cos\alpha & 0 \\ 0 & 0 & 1 \end{bmatrix} \begin{bmatrix} u_x \\ u_y \\ \omega \end{bmatrix}, \quad (5)$$

where α is the orientation of the body frame with respect to the ground frame, $\begin{bmatrix} \dot{x} & \dot{y} & \dot{\alpha} \end{bmatrix}^T$ is the UAV velocity vector with respect to the ground frame, and $\begin{bmatrix} u_x & u_y & \omega \end{bmatrix}^T$ is the UAV velocity vector with respect to its body frame. The complete the dynamic

models of the both types of rotorcrafts are presented in detail in (Raffo et al., 2010; Brandão et al., 2013).

3 LINE FOLLOWING CONTROLLER

This Section presents the design of the line following controller for the UAV. Here, we consider that the x axis of the ground frame is aligned with the line to be followed by the aircraft. Figure 3 shows a frame of a video taken from the UAV downwards camera. The UAV should follow a path which is parallel to the line, therefore the orientation error in the image frame is given by α, while the displacement error is represented by $\tilde{y}$. The line to be followed by the UAV is generated by the line detection algorithm described in Section 4. Here, such line represents the boundary between the grass and the water channel.

The control objective is to minimize both the displacement error $\tilde{y}$ and the orientation error α. Thus,

$$\dot{\tilde{y}} = u_x \sin\alpha + u_y \cos\alpha, \text{and} \qquad (6)$$

$$\dot{\alpha} = \omega. \qquad (7)$$

We are going to show that both $\tilde{y}$ and α are reduced by applying the control signals

$$u_x = (u_{x\max} - k_x|\tilde{y}|)\cos\alpha, \qquad (8)$$

$$u_y = u_{y\max}\sin\alpha, \text{ and} \qquad (9)$$

$$\omega = -k_y\tilde{y}\left(u_x\frac{\sin\alpha}{\alpha} - u_y\frac{\cos\alpha}{\alpha}\right) - k_\alpha\alpha, \qquad (10)$$

where $k_x = \dfrac{b_1}{a_1 + |\tilde{y}|}$, $k_y = \dfrac{b_2}{a_2 + |\tilde{y}|}$ and $k_\alpha = \dfrac{b_3}{a_3 + |\tilde{\alpha}|}$ are designed to avoid saturation of control signals when $|\tilde{y}|$ is large. b_1, b_2, b_3, a_1, a_2 and a_3 are positive constants. $u_{x\max}$ and $u_{y\max}$ are the maximum translational velocities on x and y axis. Notice that
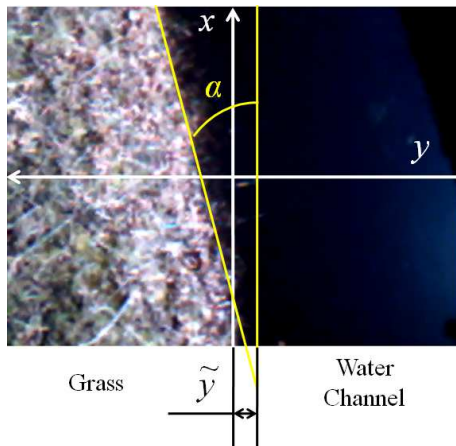
Figure 3: The line following model.

the control signals u_x, u_y and ω are directly related to f_x, f_y and τ_ψ. In closed loop, we have

$$\dot{\tilde{y}} = [(u_{x\max} - k_x|\tilde{y}|) + u_{y\max}]\sin\alpha\cos\alpha,$$

$$\dot{\alpha} = -k_y\tilde{y}\left(u_x\frac{\sin\alpha}{\alpha} - u_y\frac{\cos\alpha}{\alpha}\right) - k_\alpha\alpha. \qquad (11)$$

The stability analysis is given in the sense of Lyapunov considering the following candidate function

$$V(\tilde{y}, \alpha) = \frac{\alpha^2}{2} + \int_0^{\tilde{y}} k_y\Gamma d\Gamma. \qquad (12)$$

Taking the first time derivative and replacing (11), we have

$$
\begin{aligned}
\dot{V} &= \alpha\dot{\alpha} + k_y\tilde{y}\dot{\tilde{y}} \\
&= \alpha\left[-k_y\tilde{y}\left(u_x\frac{\sin\alpha}{\alpha} - u_y\frac{\cos\alpha}{\alpha}\right) - k_\alpha\alpha\right] \\
&\quad + k_y\tilde{y}(u_x\sin\alpha + u_y\cos\alpha) \\
&= -k_\alpha\alpha^2.
\end{aligned}
$$

Thus, one can conclude $\tilde{y}$ and α are bounded. Using La Salle theorem for autonomous systems, taking into account (11), the greatest invariant set **M** in the region

$$\Omega = \left\{\begin{bmatrix}\tilde{y} \\ \alpha\end{bmatrix} : \dot{V}(\tilde{y}, \alpha) = \mathbf{0}\right\} \Rightarrow \left\{\begin{bmatrix}\tilde{y} \\ \alpha\end{bmatrix} = \begin{bmatrix}\tilde{y} \\ 0\end{bmatrix}\right\}$$

exists only for $\tilde{y} = 0$. Therefore, the unique invariant set **M** is the equilibrium $\begin{bmatrix}\tilde{y} & \alpha\end{bmatrix}^T = \begin{bmatrix}0 & 0\end{bmatrix}^T$, which is asymptotically stable. In other words, $\tilde{y}, \alpha \to 0$ for $t \to \infty$.

The analysis above was made under the assumption of perfect sensing of the line to be followed. But, when we consider that the line detection system is not perfect, some displacement error δ_y and orientation error δ_α are added to the closed-loop equations (11). Using the same Lyapunov candidate it is possible to show that $\tilde{y}$ and α are bounded, and its bounds depend on the magnitude of the errors δ_y and δ_α.

4 LINE DETECTION

The reference for the UAV controller is generated by the line detection algorithm. The general idea consists on smoothing the image, binarizing it and identifying its main lines. Then, the main orientation is calculated as an average of the orientation of the main lines, also considering previous image frames.

A more detailed description is given as follows. First, a new frame from the video streamed by the UAV downwards camera is obtained. Then, it is converted to gray-scale and cropped (to cut-off the its
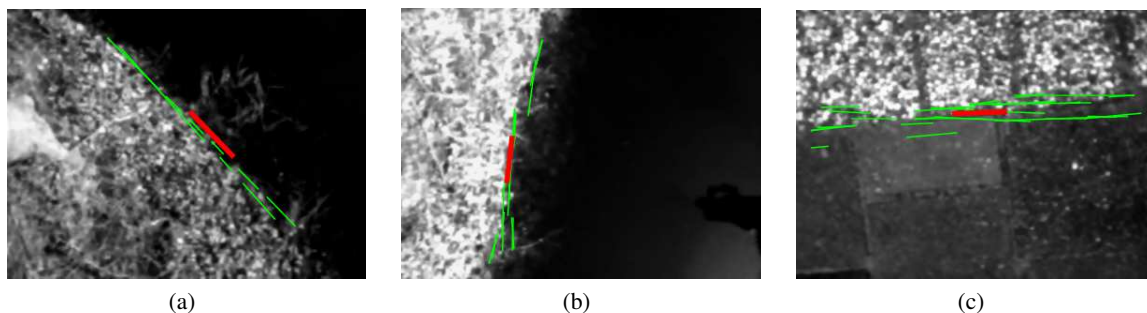
Figure 5: Examples of the application of the line detection algorithm on different conditions and surfaces: over a water channel margin (a) and (b), and over different textures of a sidewalk (c). The red line indicates the average position and orientation of the main lines detected on the previous image frames (shown in green).

Figure 4: Quadrotor used in the experiments.

black margins). The resulting image is filtered via correlation with a rotationally symmetric Gaussian low-pass filter of size 84x84 pixels with standard deviation of 28. Then, Canny method is applied to the filtered image to transform it to binary intensity image. A further convolution with the 3x3 horizontal and vertical Sobel filters is performed to emphasize borders. Then, because of its robustness to gaps and noise, standard Hough Transform is applied to the binary image, and the lines corresponding to the 10 strongest peaks in the Hough transform matrix are extracted. The orientation of those lines is computed and classified as belonging to one of four intervals in the range from 0 to 180 degrees. Only lines belonging to the interval which has the most lines are considered for the calculation of the average position and orientation in that frame. Finally, a moving average filter is used to include the information of the peak lines from the previous 5 frames on the final average. This sequence is repeated for every image frame. As a result, after each frame the position and orientation of its main lines is obtained, and this information can be used as a reference for the line following controller.

5 EXPERIMENTAL RESULTS

The quadrotor used in the experiments was the Parrot AR.Drone 2.0, shown in Figure 4 during one of the tests. It has an on-board processor that is responsible for its low-level motor control and body stabilization. Its sensors include a 3 axis gyroscope, a 3 axis accelerometer, a 3 axis magnetometer, a pressure and a ultrasonic sensors (both pressure and ultrasonic sensors are used for altitude estimation). Finally, this UAV has a 60 fps vertical QVGA camera that is used for ground speed estimation, and a 30 fps horizontal HD Camera (720p) (Parrot, 2014). Video stream from either cameras can be obtained via Wi-Fi connection to be processed on an external computer.

During our experiments we captured the video streamed by the drone downwards facing camera. Figures 5 (a) and (b) show the gray-scale frames captured in two different moments during a flight over the a water channel margin, and Figure 5 (c) illustrate the frame captured while flying over a sidewalk. In all cases, the main lines detected by the proposed algorithm are shown in green, and the average is shown in red. It can be seen that the proposed algorithm is capable of detecting the main orientation of the image pattern, and thus can generate a correct reference for the line-following controller described in Section 2. A short video is available at (Martins et al., 2015).

6 DISCUSSION

We have presented a vision-based line detection algorithm and a nonlinear line-following controller for a UAV. Stability analysis proves that the closed-loop system formed by the UAV model and the line-following controller is asymptotically stable in the sense of Lyapunov. We have also presented a vision-based strategy to detect the main lines on the images

captured by the UAV downwards camera. Experimental results using real video captured by a quadrotor UAV illustrate that the proposed algorithm is capable of determining the main position and orientation of borders such as water channel margins and different types of ground patterns.

It is important to discuss the limitations of the line detection algorithm. First, it is assumed that the images captured by the downwards camera have a pattern which contains a main orientation. Second, the proposed algorithm relies on contrast variation in order to detect lines. This is not a strong limitation since contrast variation is common in several situations, like river and channel margins, streets, etc. But, surfaces with week contrast variation are likely to cause the algorithm to perform poorly. Finally, the presence of shadows also affect the performance of the algorithm. For instance, during our experiments we noticed that shadows of tree trunks would have an important influence when they were visible in the image frame. Because the UAV is moving, we believe that the influence of shadows can be minimized with the use a of a more robust filtering method when calculating the average position and orientation of the main lines.

This work is part of a research that aims to investigate the use of UAVs in agricultural and rural areas. As an immediate next step we intend to integrate the line follower controller and the line detection algorithm for the quadrotor to fly autonomously. We also plan on integrating the proposed system to the multi-robot control scheme we have presented in (Rampinelli et al., 2010; Brandão et al., 2010; Brandão et al., 2015) to have the quadrotors flying in formation, also cooperating with a ground vehicle.

ACKNOWLEDGEMENTS

REFERENCES

Brandão, A., Sarapura, J., Caldeira, E., Sarcinelli-Filho, M., and Carelli, R. (2010). Decentralized control of a formation involving a miniature helicopter and a team of ground robots based on artificial vision. In *IEEE Latin American Robotics Symposium (LARS)*.

Brandão, A. S., Rampinelli, V. T. L., Martins, F. N., Sarcinelli-Filho, M., and Carelli, R. (2015). The multilayer control scheme: A strategy to guide n-robots formations with obstacle avoidance. *J Control, Autom Electr Syst*, 26(3):201–214.

Brandão, A. S., Sarcinelli-Filho, M., and Carelli, R. (2013). High-level underactuated nonlinear control for rotorcraft machines. In *IEEE International Conference on Mechatronics*, Vicenza, Itália.

Martins, F. N., Brandão, A. S., and Soneguetti, H. B. (2015). A Vision-based Line Following Strategy for an Autonomous UAV. Available at http://youtu.be/gd9LFQkHG28.

Parrot (2014). AR.Drone 2.0 Technical Specifications. Available at http://ardrone2.parrot.com/ardrone-2/specifications/.

Raffo, G. V., Ortega, M. G., and Rubio, F. R. (2010). An integral predictive/nonlinear $\mathcal{H}_\infty$ control structure for a quadrotor helicopter. *Automatica*, 46:29–39.

Raffo, G. V., Ortega, M. G., and Rubio, F. R. (2011). Nonlinear h-infinity controller for the quad-rotor helicopter with input coupling. In *Proceedings of the 18th IFAC World Congress*, volume 18, pages 13834–13839.

Rampinelli, V., Brandão, A., Sarcinelli-Filho, M., Martins, F., and Carelli, R. (2010). Embedding obstacle avoidance in the control of a flexible multi-robot formation. In *IEEE Int. Symp. on Industrial Electronics (ISIE)*, pages 1846–1851.

Roebuck, K. (2012). *Location-Based Services (LBS): High-impact Strategies-What You Need to Know: Definitions, Adoptions, Impact, Benefits, Maturity, Vendors*. Emereo Publishing.

Sotomayor, J. F., Gómez, A. P., and Castillo, A. (2014). Visual control of an autonomous aerial vehicle for crop inspection. *Revista Politécnica*, 33(1).

Tokekar, P., Vander Hook, J., Mulla, D., and Isler, V. (2013). Sensor planning for a symbiotic uav and ugv system for precision agriculture. *Technical Report - Dep. Comp. Science and Eng., University of Minnesota*.

Venugopalan, T., Taher, T., and Barbastathis, G. (2012). Autonomous landing of an unmanned aerial vehicle on an autonomous marine vehicle. In *Oceans, 2012*.

Warren, M., Corke, P., and Upcroft, B. (2015). Long-range stereo visual odometry for extended altitude flight of unmanned aerial vehicles. *The International Journal of Robotics Research*.